

## 3 Estimating current clear sky diurnal cycles

### 3.1 Assumptions

The developed method for estimating clear sky diurnal cycles of brightness temperatures measured from the channel  $IR_{108}$  is based on the following six major assumptions. Similar assumptions have been made for the “time contrast test” and the method to construct “IR clear-sky composites” for the ISCCP cloud detection scheme developed by *Rossow and Garder* [1993a].

#### 3.1.1 $BT_{108}$ is mainly affected by the target temperature

The measured brightness temperature  $BT_{108}$  is assumed to be mainly affected by the target temperature. As described from section 2.4.1 to section 2.5.1, the differences of  $BT_{108}$  and the temperature of an opaque target are only induced by relatively weak water absorption (figure 2-8, figure 2-9) and target emissivities differing slightly from unity (figure 2-7, figure 2-12), while other effects are negligible. Due to signal saturation at a cloud total water path of approximately  $80 \text{ g/m}^2$  (for the example shown in figure 2-16), in this context most clouds can be assumed to be opaque at  $10.8 \mu\text{m}$ .



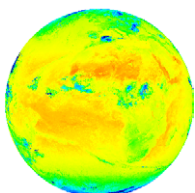
Surfaces at  $10.8\ \mu\text{m}$  generally hold emissivities in the range of 0.94 to 0.99 (figure 2-7). The emissivity of opaque clouds may be assumed to be unity (figure 2-12). Therefore, according to figure 2-5 clouds show about  $0.5\text{K}$  to  $3.5\text{K}$  higher brightness temperatures in this channel than surfaces of the same temperature.

From all gaseous atmospheric constituents, mainly water vapor affects  $BT_{108}$  (figure 2-9). The signal sensitivity to the water vapor content amounts approximately to  $-0.3\text{K}/(\text{g}/\text{m}^2)$  for dry atmospheres and  $-2.0\text{K}/(\text{g}/\text{m}^2)$  for atmospheres with  $5\ \text{g}/\text{m}^2$  integrated water vapor content. The best expectable accuracy of the clear sky estimation algorithm strongly depends on these values.

### 3. 1. 2 $BT_{108}$ is a measure for the cloud free probability

It is assumed, that the measured brightness temperature  $BT_{108}$  is a measure for the cloud free probability at each specific SEVIRI pixel and a specific moment, meaning that the appearance of a cloud is assumed to reduce the corresponding clear sky value of  $BT_{108}$ . This assumption often applies, because atmospheric temperature profiles are often monotonically decreasing with height (in the range where clouds occur) and  $BT_{108}$  approximates the target temperature (section 3. 1. 1).

Temperature inversions relative to the surface which often occur at nighttime (figure 3-1) conflict with this assumption, since they can result in  $BT_{108}$  values of clouds that are higher than the corresponding values of cloud free pixels. As this is an important possible source of error, 8400 temperature profiles measured by radiosondes from February, 1<sup>st</sup> 2004 to May, 5<sup>th</sup> 2004, distributed world wide but over represented at land in Europe, have been analyzed to quantify the frequency and the strength of those surface temperature inversions. All analyzed radiosonde data has been obtained from the NOAA online radiosonde database [Schwartz and Govett, 1992]. To allow conclusions on diurnal behaviours, the radiosonde launching times have been converted to local mean time. The calculated parameter “inversion strength” was defined as the maximum



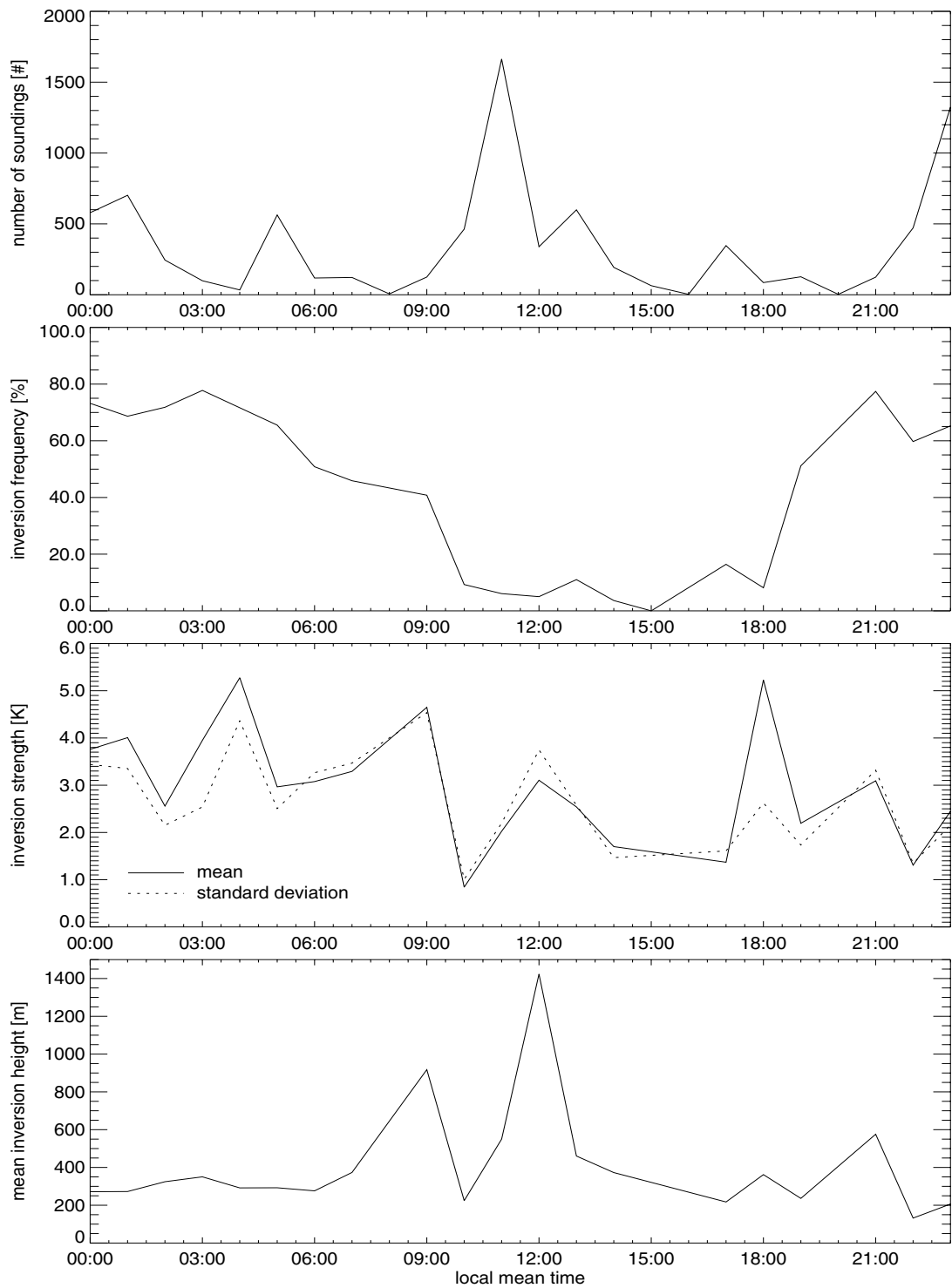


**Figure 3-1:** Statistics of surface inversions derived from 8400 radio soundings world wide from February, 1<sup>st</sup> 2004 to May, 5<sup>th</sup> 2004.



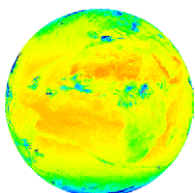
temperature inversion in respect to the  $2m$  temperature which is the first temperature value of each radio sounding. From this parameter, averages as well as standard deviations per hour (local mean time) have been calculated. The inversion height was defined as the height over ground of the inversion maximum. The results are illustrated in figure 3-1. At nighttime the inversion probability was up to 80% compared to noon time with less than 10%. The mean inversion strength ranged between  $0.8K$  and  $5.2K$  at similar standard deviations, both without an observable diurnal cycle. For the mean inversion height values between  $70m$  and  $1420m$  have been determined suggesting a diurnal cycle with its maximum around noontime. When interpreting figure 3-1 it has to be considered, that there are different radiosonde stations involved at different times of day and that the temporal data density is not constant. This may distort the shown results. Summarizing all analyzed temperature profiles leads to results given in table 3-1. As these inversions are inconsistent with the assumption above, their strength and frequency have to be considered in particular in reference to the quality of the developed assumed clear sky brightness temperature estimation algorithm.

frequency of radio soundings with surface inversions	mean inversion strength	standard deviation of inversion strength	mean height of inversion maximum
40%	$2.9K$	$2.8K$	$287m$

**Table: 3-1:** Summarized statistic of surface inversions derived from 8400 radio soundings world wide from February, 1<sup>st</sup> 2004 to May, 5<sup>th</sup> 2004.

### 3. 1. 3 Smooth surface temperature diurnal cycles

It is assumed, that the surface temperature and hence the clear sky brightness temperature diurnal cycles have a smooth hour-to-hour temporal progression with limited maximal gradients. In order to confirm this, in section 2. 6. 1 several exemplary diurnal cycles have



been analyzed, chosen under the guideline to be 24 hours cloud free. The maximum hour-to-hour temperature gradients for land and sea surfaces derived from the shown diurnal cycles (figure 2-23) are also given in section 2. 6. 1.

#### **3. 1. 4 Smooth surface temperature extra-diurnal time series**

For the developed estimation algorithm, it is also assumed, that the diurnal cycles of the surface temperatures change slowly and smoothly in the range of some days. Meaning that the gradient within the day-to-day temporal progression of the surface temperature at a certain time of day (the extra-diurnal time series introduced in section 2. 6. 2) is also limited. The exemplary extra-diurnal time series illustrated in figure 2-24 as well as the corresponding maximum day-to-day gradients for land and sea also given in this section are supposed to strengthen this assumption.

#### **3. 1. 5 Clouds cause high gradients in time series**

It is assumed that the appearance of opaque clouds generally causes gradients in the intra- as well as in the extra-diurnal time series exceeding the maximum gradients mentioned above. The vertical temperature gradient in the troposphere is generally in the range of  $-0.5$  and  $-1.0K$  per  $100m$  [Roedel, 1992]. Applying this extremely simplified temperature profile leads to the approximation that clouds in only  $1000m$  height are  $5$  to  $10K$  colder than the surface beneath. Comparing these values to the temperature gradients derived in section 2. 6. 1 and section 2. 6. 2 approves this assumption, particularly for sea surfaces.

#### **3. 1. 6 Availability of sufficient clear sky cases**

Another essential condition for reliable estimations of current clear sky brightness temperature diurnal cycles is naturally that there are statistically enough clear sky measurements at each pixel available to make the interpolation of missing values possible.



The amount of data required to estimate a pixel's diurnal cycle is not universally definable, as it strongly depends on its characteristics and its temporal variability. Especially those land pixels that have a highly variable diurnal cycle of surface temperature and that are due to their geographic location frequently cloud covered are therefore critical.

## 3.2 Estimation algorithm

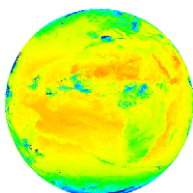
The estimation algorithm is supposed to find a most recent diurnal cycle of clear sky brightness temperatures containing the highest values per time of day and to find interpolated values for those time slots where the measured values oppose one of the assumptions above. Up-to-dateness often stands in contrast to retain highest values. Choosing the intra- and extra-diurnal thresholds has to be done in respect to this (section 3.2.2).

### 3.2.1 Operation sequence

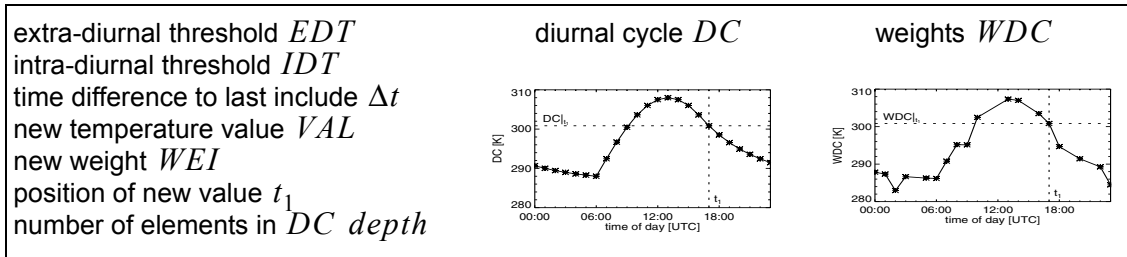
Following the assumed clear sky brightness temperature estimation (ACSBTE) algorithm flowchart (figure 3-2), the procedure to include a new temperature value  $VAL$  and a corresponding weight  $WEI$  at the position  $t_1$  in the diurnal cycle will be described in the following:

Calling the ACSBTE procedure starts the input operation. From this procedure the INSERT procedure is called.

For each pixel an array holding the up-to-date diurnal cycle  $DC$  and an array of the same size holding the corresponding weights  $WDC$  are needed. Both arrays are filled with a large negative no data value when initialized.



Global variables



$ACSBTE(DC, WDC, VAL, WEI, t_1, depth, EDT, IDT, \Delta t)$

Reduce old weights according to (3-2)	
Is the new weight greater than the old one? $WEI \geq WDC _{t_1}$	
no	yes
Initialize $t_0$ and $t_2$ according to (3-3)	
Insert $(t_0, t_2)$	

$INSERT(t_0, t_2)$

Do $t_0$ and $t_2$ still have valid values? $t_0 \neq t_2$				
no		yes		
Re-initialize $WDC$ (3-1)	Is $G_0$ of valid size (3-4)? $G_0 \leq IDT$			
	no		yes	
Set $DC$ to the constant value $VAL$	$WEI \geq WDC _{t_0}$		Is $G_2$ of valid size (3-6)? $G_2 \leq IDT$	
	no	yes	no	yes
$WDC _{t_1} = WEI$	Decrease $t_0$ (3-5)	$WEI \geq WDC _{t_2}$		Interpolate $DC$ within $]t_0, t_1[$ and $]t_1, t_2[$ (3-8)
	$INSERT(t_0, t_2)$	no	yes	
		$INSERT(t_0, t_2)$	Increase $t_2$ (3-7)	Re-initialize $WDC$ within $]t_0, t_1[$ and $]t_1, t_2[$ (3-1)
	no		yes	
$WDC _{t_1} = WEI$				

Figure 3-2: Flowchart of the ACSBTE algorithm.



$$\begin{aligned}
 DC|_* &= -10000 \\
 WDC|_* &= -10000
 \end{aligned}
 \tag{3-1}$$

Every time a new value  $VAL$  is supposed to be included in  $DC$  at a certain point of time  $t_1$ , two additional temporary variables  $t_0$  and  $t_2$  are needed. The number of time slots and therefore the size of the arrays  $WDC$  and  $DC$  is stored in the variable  $depth$ .

Every include operation starts with reduction of the weights depending on the extra-diurnal threshold  $EDT$  and the time difference  $\Delta t$  between the last included and the current dataset.

$$WDC = \begin{cases} WDC - \Delta t \cdot EDT & ;\text{if } WDC > -10000 + \Delta t \cdot EDT \\ -10000 & ;\text{otherwise} \end{cases}
 \tag{3-2}$$

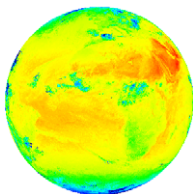
Further operations only occur if the new temperature is higher than the corresponding weight which also represents a temperature value ( $VAL \stackrel{?}{\geq} WDC|_{t_1}$ ). This ensures that extra-diurnal time series of the estimated assumed clear sky brightness temperature can only decrease smoothly. Suitable values for  $EDT$  will be given in section 3. 2. 2.

Considering periodic array boundaries (by applying the modulo operator),  $t_0$  and  $t_2$  are initialized with points in time surrounding  $t_1$  :

$$\begin{aligned}
 t_0 &= (t_1 + depth - 1) \bmod depth \\
 t_2 &= (t_1 + 1) \bmod depth
 \end{aligned}
 \tag{3-3}$$

These values are passed to the recursive INSERT procedure that is supposed to insert the new temperature value in the current diurnal cycle in a way which best possibly satisfies the assumptions of section 3. 1.

First of all, the INSERT procedure checks if the values of  $t_0$  and  $t_2$  are valid. This is only true if they differ from each other, so that there is still the possibility to find an updated diurnal cycle with gradients less than the intra-diurnal threshold  $IDT$ .



If  $t_0$  equals  $t_2$  it is not possible to preserve any old value of the current  $DC$  array without opposing the assumption of smooth diurnal cycles (section 3. 1. 3). This only happens if  $VAL$  is much larger than every value of  $WDC$ , indicating that  $VAL$  is either the first non-cloud-affected measurement or much newer than every  $WDC$  value. Consequently,  $WDC$  is re-initialized according to (3-1): every  $DC$  value is set to  $VAL$ , and the weight of the current position  $WDC|_{t_1}$  is set to the new weight  $WEI$ . Setting the whole diurnal cycle to a constant value is certainly not very realistic, but this approximation represents the only available information. Setting all  $WDC$  values except one to the initialization value ensures that the following values may easily be included.

In the other case, if  $t_0$  and  $t_2$  differ, the gradient  $G_0$  between  $t_0$  and  $t_1$  within the potential new  $DC$  array is calculated:

$$G_0 = |(DC - VAL) / ((t_1 - t_0 + depth) \bmod depth)| \quad (3-4)$$

If  $G_0$  exceeds the intra-diurnal threshold  $IDT$  a comparison between  $VAL$  and  $WDC|_{t_0}$  is performed. In the case  $VAL < WDC|_{t_0}$ , the new temperature value will be rejected and no changes to the diurnal cycle occur, as it is not possible to include the new temperature value into the current diurnal cycle without neglecting the assumptions of section 3. 1. 3 or section 3. 1. 4. In the other case ( $WEI \geq WDC|_{t_0}$ )  $t_0$  is decreased by one time interval:

$$t_0 = (t_0 + depth - 1) \bmod depth \quad (3-5)$$

Then the INSERT procedure is recursively called with the new value of  $t_0$ .

If  $G_0 \leq IDT$ ,  $t_0$  will not be changed anymore and the algorithm tries to find an adequate value for  $t_2$  in an analog way by calculating the gradient

$$G_2 = |(DC|_{t_2} - VAL) / ((t_1 - t_2 + depth) \bmod depth)|, \quad (3-6)$$

comparing it to  $IDT$  and if necessary by increasing  $t_2$

$$t_2 = (t_2 + 1) \bmod depth \quad (3-7)$$



with following recursive calling of the insert procedure.

In the case of  $G_0$  and also  $G_2$  are less equal  $IDT$  the updated diurnal cycle is calculated by linear interpolation within the interval  $]t_0, t_1]$  and  $[t_1, t_2[$  as followed:

$$DC|_{t_i} = DC|_{t_1} + (DC|_{t_{0/2}} - DC|_{t_1}) \cdot \frac{(t_1 - t_i + depth) \bmod depth}{(t_1 - t_{0/2} + depth) \bmod depth} \quad (3-8)$$

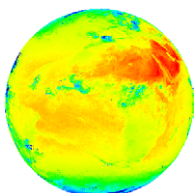
In this equation,  $t_i$  represents an arbitrary position between  $t_1$  and  $t_{0/2}$ . If  $t_0$  or  $t_2$  is adjacent to  $t_i$ , interpolation on this side is naturally not required. Furthermore,  $WDC$  is re-initialized according to (3-1) within these intervals to ensure easy including of new values. Anyway,  $DC|_{t_1}$  and  $WDC|_{t_1}$  will be set to the new values.

By means of this insert method the new calculated diurnal cycle is more recent and still fulfilling the assumptions above.

Inserting should only be performed, if the time of day of the new value belongs to an integer position value in respect to  $depth$ . E.g. when choosing a  $depth$  value of 24, only every fourth of 96 MSG images per day should be inserted. When reading estimated clear sky values of arbitrary time of day representing non-integer positions, linear interpolation between the neighboring time positions is performed.

The estimation algorithm was also designed considering computational aspects: In order to optimize calculation performance, all interpolation operations have been reduced to 16bit integer operations. In order to minimize hard disk input/output, all temperature data on the hard disk is represented by byte values only. As a consequence, the accuracy of all stored and calculated temperature values has been reduced to 0.5K because of temperature scaling to the dynamic range of byte values.

Just like the whole cloud detection algorithm, the ACSBTE algorithm was designed to take advantage of IDL's fast array operations. In order to prevent data loss due to computer crashes and to avoid memory lack, all  $DC$  and  $WDC$  data is saved to disk when not in use. With its universal design, the diurnal cycle estimation algorithm is easily portable for use with other data and satellites as long as the assumptions made in section 3. 1 are satisfied.



### 3. 2. 2 Defining constants

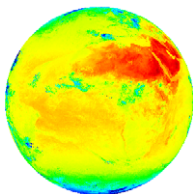
For the intra-diurnal gradient thresholds  $IDT$ , best results have been obtained when choosing values close to the maximum measured gradient values (figure 2-23). The value for land surfaces was set to  $6.5 K/h$  at a maximum measured value of  $7 K/h$  (section 2. 6. 1). For sea surfaces, the  $IDT$  value was set to  $0.75 K/h$  compared to a maximum measured value of  $1 K/h$ . These values are used for all experiments concerning the estimation of diurnal cycles as well as for operational cloud detection. Significantly larger values could lead to misinterpretation of cloud induced brightness temperature changes as rapid changes of the surface temperature. Choosing too small values for  $IDT$  would make estimation of correct clear sky diurnal cycles impossible. Estimation of systematically too large temperature values and diurnal cycles with too small amplitudes would be the consequence.

As the extra-diurnal time series maximum gradient threshold  $EDT$  reduces the weights  $WDC$  (3-2), it basically corresponds to the temporal steadiness of the estimated diurnal cycles. Setting  $EDT$  to zero would correspond with infinite recollection so that only maximum values would be stored. This could only produce applicable results in periods of continuous surface warming. In particular for pixels which are statistically rarely cloud free, the probability of including cloudy cases in the estimated clear sky diurnal cycles increases by choosing too large  $EDT$  values. For all experiments concerning the estimation of diurnal cycles as well as for operational cloud detection, the  $EDT$  values have been set to  $2 K/day$  for pixels over sea and to  $4 K/day$  for pixels over land surfaces. Both values are in the range of the corresponding mean and maximum values of  $1 K/day$  to  $3.3 K/day$  for the investigated sea surfaces and  $2 K/day$  to  $7.8 K/day$  for the investigated land surfaces (section 2. 6. 2).  $EDT$  and  $IDT$  alike, have been defined only land/sea dependent. A finer separation in different land usage classes has been rejected to avoid dependencies on external data.



With MSG's temporal resolution of 15 minutes, only *depth* values less equal 96 are reasonable. Large *depth* values enable a more accurate registration of small scale diurnal cycle features but they also significantly increase calculation expense and amount of hard disk input/output. In the case of small *depth* values, less data with larger time differences can be included in the consequence that minor, but abrupt temperature changes, caused by warm clouds are harder to detect. Setting *depth* to 24 instead of the maximum value 96, reduces the computation time for including one MSG image from 570s to 148s (PC with AMD Athlon2200+ CPU), furthermore only 24 instead of 96 include operations have to be performed per day. Figure 3-3 shows the behavior of convergence between two experiments with *depth* = 24 and *depth* = 96, respectively. Both experiments have been initialized on January, 25<sup>th</sup> 2004, 00:00 UTC and ended nine days later on February, 2<sup>nd</sup> 2004, 23:45. Illustrated are the mean brightness temperature difference of the estimated clear sky images, the average of the absolute temperature difference, and the corresponding standard deviation. All of the three graphs suggest, that remarkable increasing of accordance only occurs within the first five days. After this time the mean estimation difference amounts to  $-0.2 K$  (in average) ranging from  $-0.4 K$  to  $0.0 K$ , the mean absolute difference amounts to  $0.8 K$  (in average) ranging from  $0.5 K$  to  $1.1 K$ , and the standard deviation of the temperature difference amounts to  $1.9 K$  (in average) ranging from  $1.5 K$  to  $2.3 K$ . In the case of *depth* = 24, three of four images are only the result of an interpolation but not of an input operation. This fact causes the high-frequency fluctuations in figure 3-3. Supposing that the experiment with *depth* = 96 results in more realistic diurnal cycles, these values might be utilized for estimating the error of the algorithm with *depth* = 24. Due to considerable differences in computation time, *depth* has been set to 24 for every further experiment concerning the estimation of diurnal cycles as well as for operational cloud detection.

Table 3-2 summarizes the values *IDT*, *EDT*, and *depth* which have been determined in this section to be suitable for operational cloud detection.



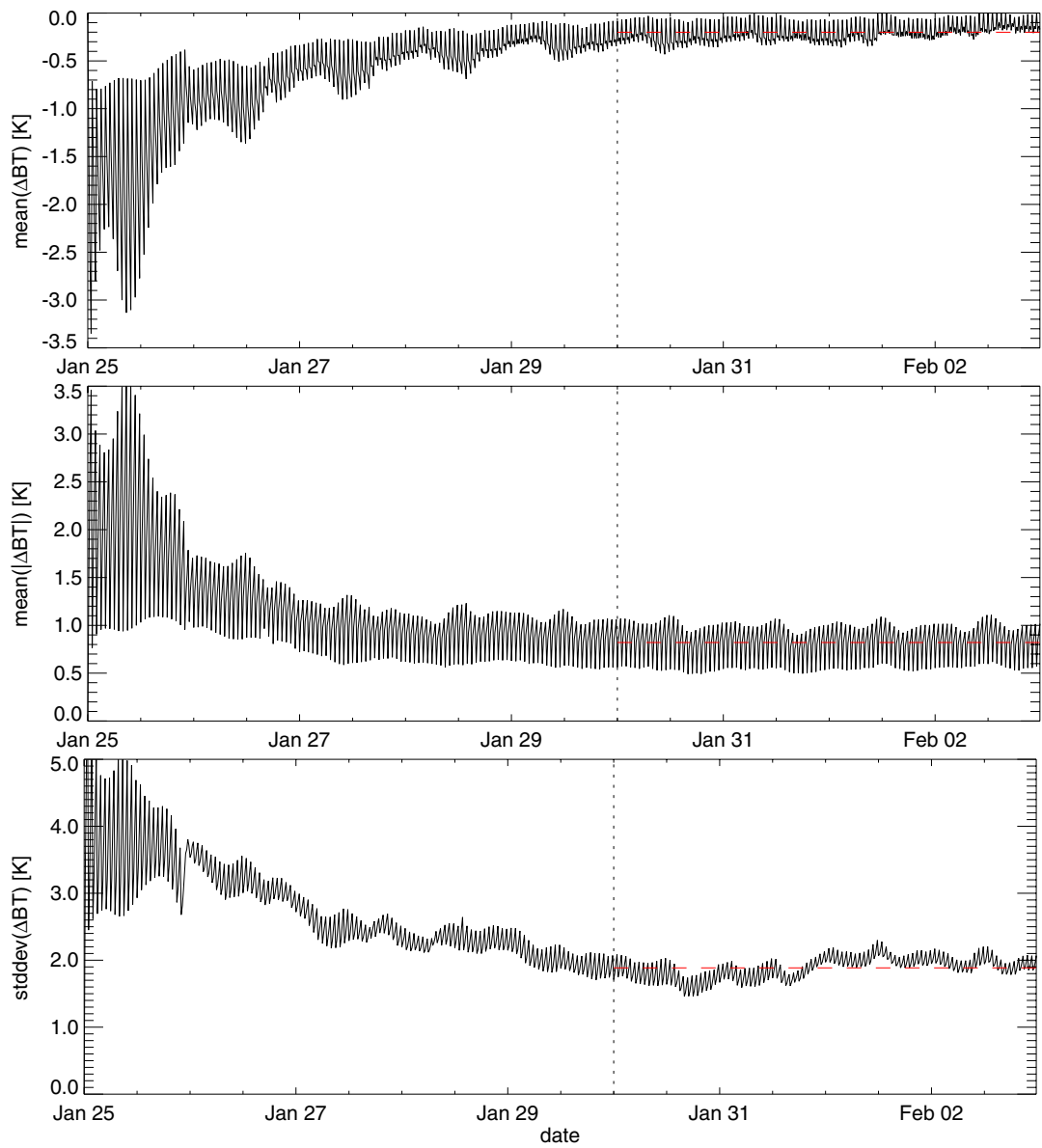


**Figure 3-3:** Analysis of the difference in the assumed clear sky brightness temperature calculated by the ACSBTE algorithm with *depth* set to 24 and 96, respectively. Illustrated are, from January, 25<sup>th</sup> 2004, 00:00 UTC to February, 2<sup>nd</sup> 2004, 23:45 UTC, the mean difference (top), the mean absolute difference (middle), and the standard deviation (bottom). Extra highlighted is the region after a spin-up time of five days. The red dashed lines represent the average values of these regions.



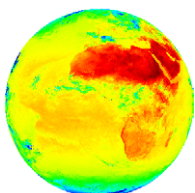
intra-diurnal threshold $IDT$ [K/h]		extra-diurnal threshold $EDT$ [K/day]		$depth$
land	see	land	see	
6.50	0.75	4.00	2.00	24

**Table: 3-2:**  $IDT$ ,  $EDT$ , and  $depth$  values as chosen for operational cloud detection.

### 3. 2. 3 Remarks

Naturally, the developed method is not restricted to data from channels around  $10.8\mu m$  only. It rather might be utilized for all data satisfying the assumptions in section 3. 1. But due to its characteristics, which were discussed in detail in chapter 2,  $BT_{108}$  best fulfills these assumptions. Referring to section 3. 1. 1,  $BT_{120}$  and  $BT_{134}$  are less useful as they are more affected by water vapor absorption (figure 2-9).  $BT_{087}$  is highly affected by different potential target emissivities (figure 2-7, figure 2-12). This fact also opposes the first assumption. In contrast to the third assumption (section 3. 1. 3), the impact of solar radiation causes discontinuities in the diurnal cycles of  $BT_{039}$  (figure 2-14). The remaining thermal channels  $IR_{097}$ ,  $IR_{073}$ , and  $IR_{062}$  are not taken into consideration because of their major sensitivities to water vapor and ozone (figure 2-9), respectively. Analog assumptions aimed at estimating clear sky reflectivities from a channel in the visible spectral region at daytime have been formulated. Very low reflectivity values in regions of cloud shadows pretend very low surfaces reflectivities which leads to corrupted results.

The use of land/sea surface temperature products instead of  $BT_{108}$  does not seem to be reasonable. These products are mostly based on split window methods utilizing the temperature difference  $BT_{108} - BT_{120}$  to correct for water vapor absorption. Interpreting this value is ambiguous, as thin clouds may produce similar values (figure 2-17) like cloud free atmospheres with a high amount of water vapor do (figure 2-18).



### 3. 3 Estimation quality

Two experiments have been accomplished in order to assess the stability and quality of the developed estimation method.

To prove the stability and to estimate the spin-up time needed to achieve suitable results, a reference run initialized on January, 1<sup>st</sup> 2004 covering SEVIRI's entire field of view has been compared to five test runs consecutively initialized with two week intervals on February, 15<sup>th</sup> 2004, February 29<sup>th</sup> 2004, March, 14<sup>th</sup> 2004, March, 28<sup>th</sup> 2004, and April, 11<sup>th</sup> 2004. All runs have been terminated at the end of April 2004. The mean difference of the estimated assumed clear sky brightness temperatures as well as the mean absolute difference and the standard deviation of the temperature difference are graphed in figure 3-4. First of all, from this illustration can be concluded, that after spin-up time all test runs converge against the reference run so that the obtained results are basically independent on the initialization date. This behavior is an important stability criterion. By means of this experiment the spin-up time can be estimated. Averaged over the five test runs table 3-3 shows values of the three parameters illustrated in figure 3-4 for different spin-up times. According to table 3-3, for the purpose of cloud detection a spin-up time of five to ten days seems to be sufficient. Hence, a quality index, calculated from the up-to-dateness and the amount of data used for deriving diurnal cycles, has been defined, ensuring that only adequate estimated assumed clear sky brightness temperature data is taken into account.

The second experiment is the comparison between estimated assumed clear sky temperatures and brightness temperatures calculated with XTRA. For this purpose, 7301 temperature/humidity profiles of cloudy as well as cloud free atmospheres measured by radiosondes in the period from February, 11<sup>th</sup> 2004 to May, 31<sup>st</sup> 2004, distributed over SEVIRI's full field of view but over represented at land in Europe have been utilized as



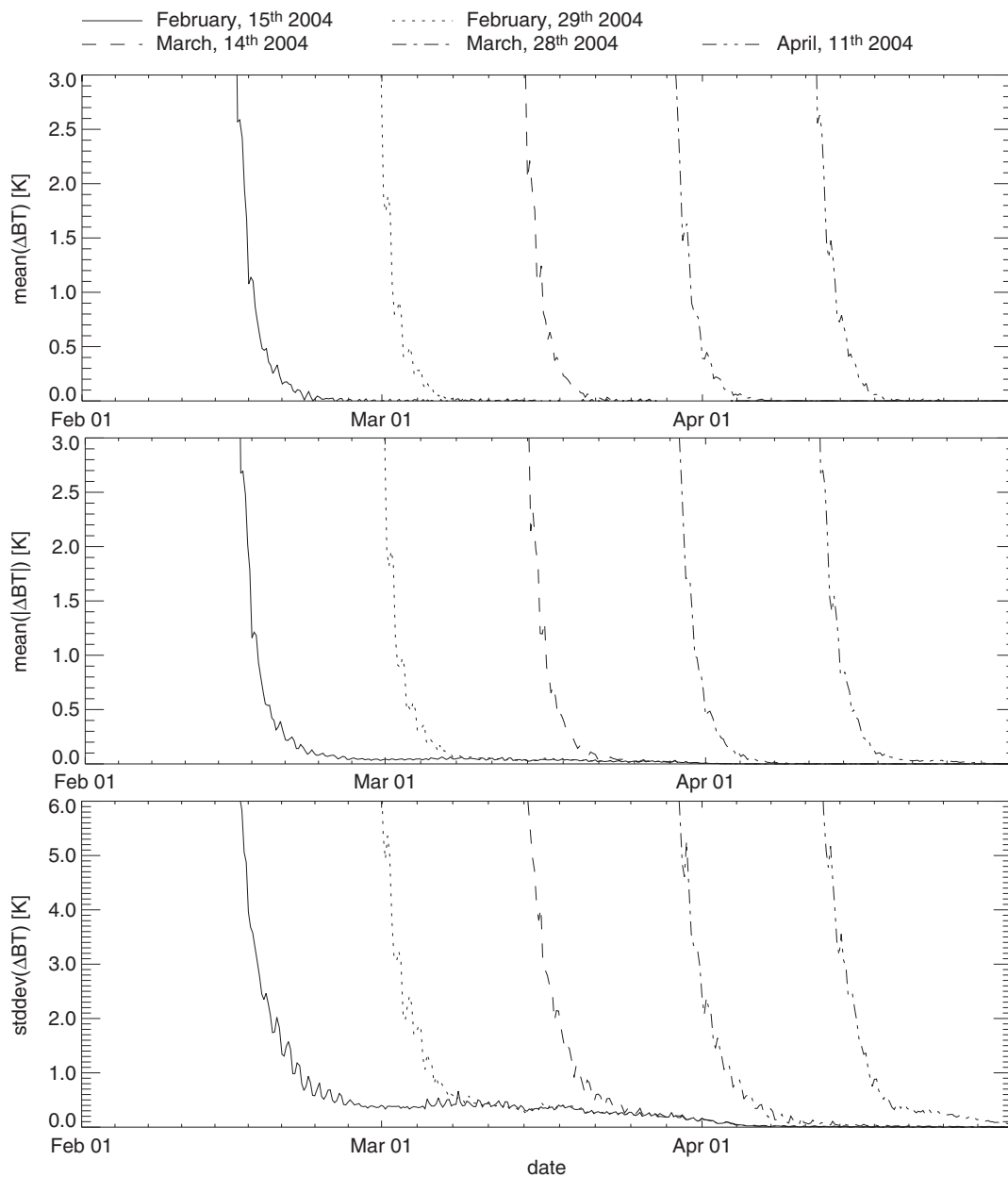
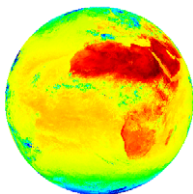


**Figure 3-4:** This figure investigates the spin-up phase of five test runs of the ACSBTE algorithm initialized on February, 15<sup>th</sup> 2004, February, 29<sup>th</sup> 2004, March, 14<sup>th</sup> 2004, March, 28<sup>th</sup> 2004, and April, 11<sup>th</sup> 2004, covering SEVIRI's entire field of view. All test runs are compared to a reference run initialized on February, 1<sup>st</sup> 2004 by analyzing  $\Delta BT = BT_{test} - BT_{reference}$ . The mean brightness temperature difference (**top**), the mean of the absolute difference (**middle**), and the standard deviation of the difference (**bottom**) are illustrated for all SEVIRI pixels .



spin-up time [days]	mean( $\Delta BT$ ) [K]	mean( $ \Delta BT $ ) [K]	stddev( $\Delta BT$ ) [K]
5	0.19	0.25	1.56
10	0.007	0.04	0.43
15	0.002	0.02	0.24

**Table: 3-3:** Averaged over the five test runs, this table gives dependent on the spin-up time values for the parameters shown in figure 3-4.

input for XTRA radiative transfer simulations. The lowermost temperature value of each radiosonde profile which corresponds to the air temperature at a height of  $2m$  above ground, has been used as approximation for the surface temperature. The surface emissivity has been set to unity. Independent of the actual cloud coverage, for each temperature/humidity profile one cloud free radiative transfer simulation was performed. The results of these simulations have been compared to the corresponding values estimated by the ACSBTE algorithm initialized on February, 1<sup>st</sup> 2004. Figure 3-5 shows the mean and the standard deviation of the difference  $BT_{ACSBTE} - BT_{XTRA}$ . Illustrated are the overall diurnal cycle on a three-hourly basis and the temporal progression within the whole period on a daily basis, including only those days with more than 50 radio soundings. The overall mean and standard deviation amounts to  $-0.8K$  and  $6.8K$ , respectively. Additionally, this figure includes a two-dimensional histogram, quantifying the overall accordance between the estimated and the simulated values. The corresponding linear fit has a slope of 1.26, indicating an overestimation of large values and an underestimation of small simulation values. This discrepancy does not have to be necessarily attributed to the ACSBTE algorithm, as the signal of  $BT_{108}$  has its major sensitivity to the surface (skin) temperature (figure 2-15) that can differ due to surface heating/cooling effects from the  $2m$  temperature measured by the radiosonde.

To summarize, it can be stated that the ACSBTE algorithm produces results with stable quality (figure 3-5, middle). The accuracy of the ACSBTE algorithm can be estimated to  $6.8K$ , the derived overall value of the standard deviation. This value can be understood as “worst case” value, because the pronounced diurnal cycle of the estimation accuracy



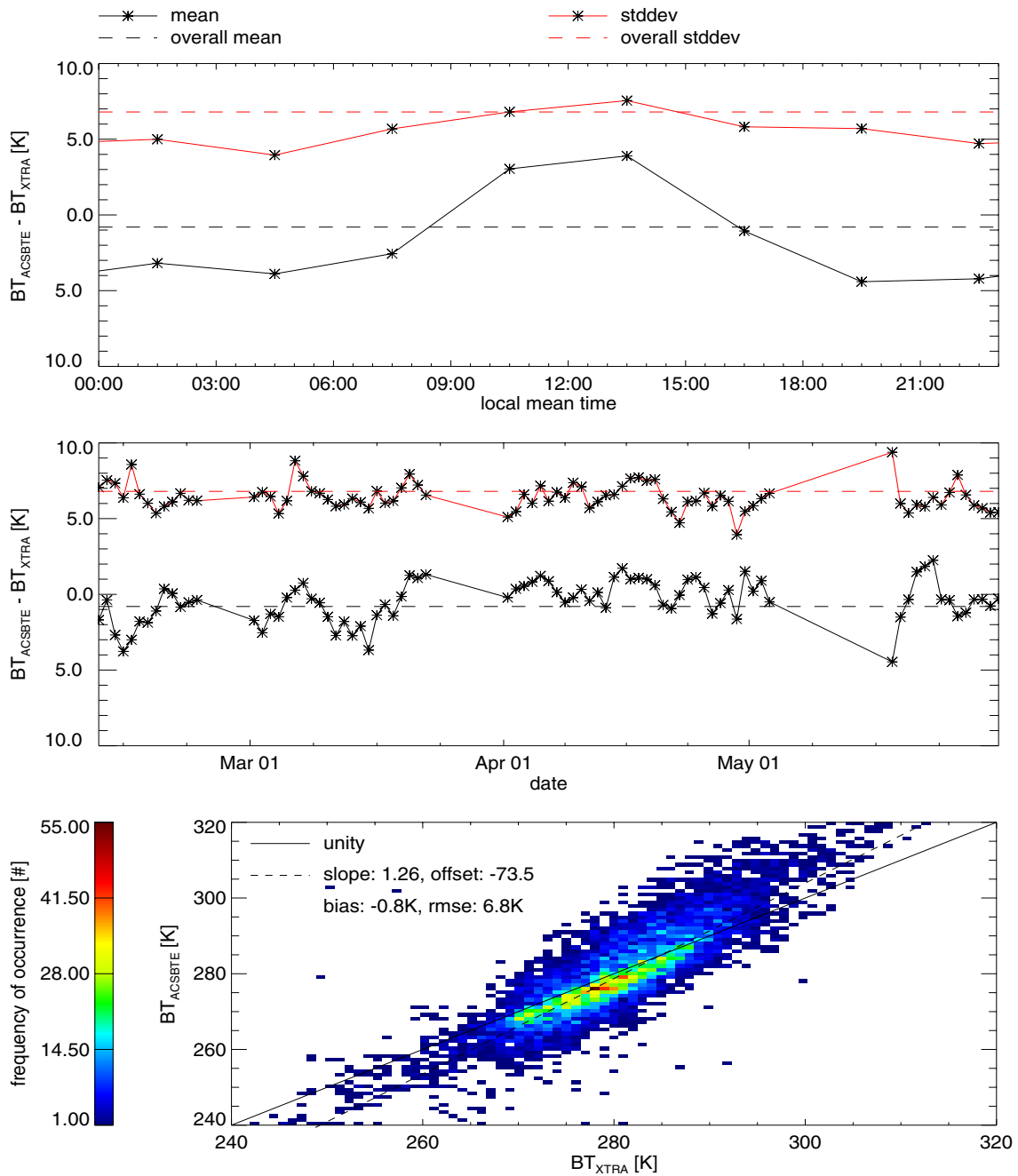
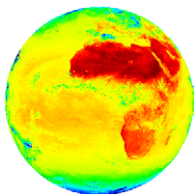


**Figure 3-5:** This figure shows the comparison of XTRA simulated  $BT_{108}$  values with corresponding assumed clear sky brightness temperatures derived by the ACSBTE algorithm. 7301 temperature/humidity profiles of cloudy and cloud free atmospheres measured by radiosondes in the period from February, 11<sup>th</sup> 2004 to May, 31<sup>st</sup> 2004, distributed over SEVIRI's full field of view but over represented at land in Europe have been used as input to XTRA simulations. **top:** Overall diurnal cycle on a three-hourly basis. **middle:** Temporal evolution on a daily basis. **bottom:** Two-dimensional histogram of accordance between  $BT_{ACSBTE}$  and  $BT_{XTRA}$  and also the corresponding linear regression (**dashed line**).



indicates that surface heating/cooling effects cannot be neglected. In order to get a more realistic estimate, it was assumed that at least 30% of the data corresponds to clear sky cases, where surface heating/cooling presumably causes the greatest differences between  $2m$  and skin temperature. Excluding 30% of the data with the largest differences between  $BT_{ACSBTE}$  and  $BT_{XTRA}$  by a percentile threshold results in a mean difference value of  $-1.0K$  and a standard deviation of  $3.3K$ . The accuracy of the clear sky brightness temperature of land surfaces of the ISCCP cloud detection scheme is specified with  $4K$  [Rossow and Garder, 1993b]. Even though the ISCCP value is also based on  $2m$  temperature measurements, the comparison is critical, because a different method was used to account for surface heating/cooling effects. In reference to the precision of the assumptions in section 3. 1. 1 and section 3. 1. 2, the estimated accuracy value of  $3.3K$  seems to be reasonable. As just a few investigated radio soundings were over sea surfaces, this value is relevant only for land surfaces. The corresponding accuracy for sea surfaces might be higher because of lower  $EDT$  and  $IDT$  values (section 3. 2. 2). The estimated clear sky temperatures will be particularly useful for detecting clouds which lower the measured top of atmosphere brightness temperature significantly more than the given accuracy.

Referring to the first experiment described in this section, it was determined that after a spin-up phase of five to ten days the ACSBTE algorithm produces reliable results. For operational cloud detection it turned out that a spin-up phase of five days is sufficient.

In individual cases, especially if one of the assumptions of section 3. 1 is not satisfied, larger errors may occur. Due to the design of this temporal-based method erroneous input data of a single date may lead to wrong results at following dates. This applies in particular to too high input temperatures  $BT_{108}$ .

The flip-book animation on the bottom of the left pages illustrates the assumed clear sky brightness temperature estimated by the ACSBTE algorithm during the first two days of a spin-up phase (May, 24<sup>th</sup> 2004, 00:00 UTC - May, 26<sup>th</sup> 2004, 23:00 UTC). Cold areas like clouds are blue, warm areas are red. The first image of the animation still shows many cold areas due to the fact that the algorithm after initialization simply takes the  $BT_{108}$



image as first guess. After only one day (approximately page 40) the very cold clouds have already been eliminated and moving structures have nearly been extinguished. Heating and cooling of desert surfaces is the main visible feature for the following two days. At the end of the animation some remaining cloud induced structures (e.g. near the equator and over the southern Atlantic ocean) indicate, that the spin-up phase has not yet been completed and that the algorithm is not inerrant. This applies especially for regions with nearly permanent cloud coverage.

